The Receptor for Advanced Glycation End Products Is Highly Expressed in the Skin and Upregulated by Advanced Glycation End Products and Tumor Necrosis Factor-Alpha

Christina Lohwasser[1,6], Daniel Neureiter[2,3,6], Bernd Weigle[4], Thomas Kirchner[2] and Detlef Schuppan[1,5]

Advanced glycation end products (AGEs) form non-enzymatically from reactions of proteins with reducing sugars. In the skin, AGEs were reported to accumulate in dermal elastin and collagens and to interact nonspecifically with the cell membrane of dermal fibroblasts. Therefore, AGEs may influence the process of skin aging. We investigated the presence of the AGE receptor RAGE in skin and the influence of AGEs on receptor expression and the formation of extracellular matrix (ECM). Sections of sun-protected and sun-exposed skin were analyzed with monoclonal antibodies against (RAGE), heat-shock protein 47, factor XIIIa, CD31, and CD45. RAGE was mainly expressed in fibroblasts, dendrocytes, and keratinocytes and to a minor extent in endothelial and mononuclear cells. Human foreskin fibroblasts (HFFs) highly expressed RAGE on the protein and mRNA level when analyzed by quantitative Western blotting and real-time PCR. Incubation of HFFs with the specific RAGE ligand N^{ε}-(carboxymethyl)lysine-modified BSA (CML-BSA) and tumor necrosis factor-alpha resulted in significant upregulation of RAGE expression. CML-BSA induced a mildly profibrogenic pattern, increasing connective tissue growth factor, transforming growth factor-beta (TGF-β)1, and procollagen-α1(I) mRNA, whereas expression of matrix metalloproteinase (MMP)-1, -2, -3, and -12 was unaffected. We conclude that in HFFs, AGE–RAGE interactions may influence the process of skin aging through mild stimulation of ECM gene expression.

Journal of Investigative Dermatology (2006) **126,** 291–299. doi:10.1038/sj.jid.5700070; published online 22 December 2005

INTRODUCTION

Advanced glycation end products (AGEs) result from non-enzymatic glycation of the amino groups of proteins with reducing sugars such as glucose. The specific AGE N^{ε}-(carboxymethyl)lysine (CML) modifies skin elastin, especially during UV-induced photoaging (Mizutari *et al.*, 1997), and AGEs accumulate on skin elastin and collagen, interfering with normal skin function (Wondrak *et al.*, 2002). Increased AGE levels in skin collagen are found during the normal process of aging, in diabetes or chronic renal failure (Schnider and Kohn, 1980, 1981; Monnier *et al.*, 1984, 1999; Dyer *et al.*, 1993; Jeanmaire *et al.*, 2001; Meng *et al.*, 2001). The formation of AGEs on skin collagen favors collagen crosslinking, resulting in decreased degradability by, for example, matrix metalloproteinases (MMPs) and impaired dermal regeneration. Okano *et al.* (2002) postulated that AGEs bind to fibroblast cell membranes, contributing to the progression of skin aging.

Receptor for AGE (RAGE), a member of the immunoglobulin superfamily of cell surface receptors, interacts with several ligands, especially with CML (Kislinger *et al.*, 1999). RAGE is expressed in a variety of tissues and cells, including cells of the vessel walls, neural tissues, cardiac myocytes, monocytes and macrophages, T-lymphocytes, and mesangial cells (Brett *et al.*, 1993; Wautier and Guillausseau, 2001). The role of RAGE in interactions of AGEs with dermal fibroblasts, especially in the context of skin aging, remains largely unclear.

During skin aging and in sun-exposed skin, the normal fibrillary pattern of dermal extracellular matrix (ECM) is

[1]*Department of Medicine I, University of Erlangen-Nuernberg, Germany;* [2]*Department of Pathology, University of Erlangen-Nuernberg, Germany;* [3]*Institute of Pathology, Landeskliniken Salzburg, Austria;* [4]*Institute for Immunology, Technical University Dresden, Germany and* [5]*Division of Gastroenterology, Beth Israel-Deaconess Medical Center, Harvard Medical School, Boston, Massachusetts, USA*

[6]*These two authors contributed equally to this work*

Correspondence: Dr Detlef Schuppan, Division of Gastroenterology, Beth Israel-Deaconess Medical Center, Harvard Medical School, 330 Brookline Avenue, Dana 502, Boston, Massachusetts 02215, USA.
E-mail: dschuppa@bidmc.harvard.edu

Abbreviations: AGE, advanced glycation end product; CML, N^{ε}-(carboxymethyl)lysine; CTGF, connective tissue growth factor; ECM, extracellular matrix; GAPDH, glyceraldehyde-3-phosphate dehydrogenase; HFF, human foreskin fibroblast; HSP, heat-shock protein; MMP, matrix metalloproteinase; PC-α1(I), procollagen-alpha1(I); RAGE, receptor for advanced glycation end products; SD, standard deviation; TGF-β, transforming growth factor-beta; TNF-α, tumor necrosis factor-alpha.

Received 14 October 2004; revised 8 June 2005; accepted 24 June 2005; published online 22 December 2005

replaced by non-functional ECM, in which the normally divalent collagen crosslinks have been replaced by trivalent crosslinks, causing thickening and tangling of collagen fibrils (Kligman and Kligman, 1986; Wulf *et al*., 2004).

The major structural components of the dermal ECM are collagen I and III, accounting for over 70 and 15%, respectively, of skin dry weight and providing the dermis with tensile strength and stability. Other structurally important skin collagens are types IV, V, VI, and XIV. Collagen metabolism is a complex process requiring balanced synthesis and degradation by, for example, MMPs, and the action of cytokines. Thus, MMP production is stimulated through tumor necrosis factor-alpha (TNF-α) released after UV exposure, leading to degradation of collagen and elastin and, hence, dermal photoaging (Lovell *et al*., 1987; Koivukangas *et al*., 1994; Brenneisen *et al*., 1996). The interstitial collagenases MMP-1 and -13 preferentially degrade collagens I and III, whereas the gelatinases MMP-2 and -9 are responsible for the breakdown of collagen IV, the major basement membrane protein, and also of collagen I when complexed with tissue inhibitor of MMP (TIMP-2) and MMP-14. MMP-3 cleaves various ECM substrates including collagen IV, proteoglycans, fibronectin, and laminin and activates other pro-MMPs (Burgeson, 1982; Brenneisen *et al*., 2002). The macrophage metalloelastase MMP-12 is responsible for the degradation of elastin and a broad range of matrix and non-matrix substrates (Chandler *et al*., 1996; Shipley *et al*., 1996; Gronski *et al*., 1997). Central profibrogenic cytokines are transforming growth factor-beta 1 (TGF-β1) and connective tissue growth factor (CTGF), a downstream mediator of TGF-β1 action.

In the present study, we investigated the influence of glycated proteins (AGEs) on skin aging by studying their influence on ECM-related gene expression in skin fibroblasts. This was correlated to expression of RAGE *in vitro* and *in vivo* and to the induction of RAGE by the proinflammatory cytokine TNF-α.

RESULTS

RAGE expressed in different human skin tissues

Comparison of sun-protected skin from younger and older patients in the same anatomical region (breast). Sun-protected skin of younger patients showed a normal morphological architecture of the cutis without the typical signs of chronological aging or photoaging (Figure 1a). Sun-protected skin from older patients displayed signs of chronological aging (Figure 1i): (1) atrophy of the epidermis and (2) hypocellularity in the papillary layer of the dermis as shown by the reduced amount of factor XIIIa-positive dendrocytes (Figure 1j), CD31-positive endothelial cells (Figure 1k), and heat-shock protein (HSP)47-positive skin fibroblasts (Figure 1m and n). The number of CD45-positive lymphocytes was increased (Figure 1l). In the skin of young donors, RAGE could be localized mainly in the superficial and middle zone of the epidermis (Figure 1g and h), whereas in the skin of older patients, RAGE was located in the middle and basal zone of the epidermis (Figure 1o). In fetal skin, RAGE was predominantly found in the upper zone of the epidermis (data not shown). In the dermis, RAGE-positive cells were mainly detected in the papillary layer of younger donors (Figure 1g and h), compared to the reticular layer in older donors (Figure 1o and p). In fetal dermis, only few cells, mainly endothelial cells, were RAGE positive (data not shown).

Comparison of sun-protected versus sun-exposed skin from older patients in different anatomical regions (knee vs face). Sun-protected skin from older patients showed atrophy of the epidermis (Figure 1q) and hypocellularity, mainly in the upper dermis, of dendrocytes (Figure 1r), vascular cells (Figure 1s), lymphocytes (Figure 1t), and skin fibroblasts (Figure 1u and v). In sun-exposed skin from older patients, typical signs of photosensitivity were observed such as deep solar elastosis (Figure 1y), scattered dendrocytes and stellate fibroblasts (Figure 1z and cc), dilation of vessels (Figure 1aa), and small aggregates of lymphoid cells (Figure 1bb). In sun-protected and sun-exposed skin, RAGE was predominantly found in the basal layer and the adjacent middle zone of the epidermis (Figure 1w, ee, and ff). Additionally, in the epidermis of sun-exposed tissues, an inhomogeneous and patchy RAGE positivity of keratinocytes was observed (Figure 1ff). In the dermis, mainly in the papillary layer, of sun-exposed skin (Figure 1ee and ff), the number of RAGE-positive cells was increased compared to sun-protected skin (Figure 1w and x). RAGE-positive cells were localized around areas of solar elastosis, but RAGE was not detectable in areas with intact extracellular matrix (Figure 1ff).

The distribution patterns of RAGE-expressing cells were semiquantified as summarized in Table 1.

Cellular expression patterns of RAGE in skin. In order to characterize RAGE-expressing cells (Figure 1g, h, o, p, w, x, ee, and ff), colocalization studies were performed by using consecutive sections counterstained for HSP47 (Figure 1e, f, m, n, u, v, cc, and dd, higher magnification), factor XIIIa (Figure 1b, j, r, and z), CD31 (Figure 1c, k, s, and aa), and CD45 (Figure 1d, l, t, and bb). In all instances (normal, aged, and sun-exposed skin), the majority of RAGE-positive cells were identified as skin fibroblasts, dendrocytes, and endothelial cells, whereas only few CD45-positive lymphocytes expressed RAGE.

Human foreskin fibroblasts express RAGE

High-level expression of RAGE by untreated human foreskin fibroblasts (HFFs) was confirmed by semiquantitative Western blotting using a monoclonal anti-RAGE antibody (Figure 2).

CML-BSA and TNF-α upregulate RAGE protein and mRNA expression

HFF were exposed to increasing concentrations of CML-BSA, lysed, and subjected to Western blotting for RAGE and β-actin. CML-BSA at 10 and 50 μg/ml upregulated RAGE protein expression more than three-fold ($P<0.05$), whereas no upregulation was found at 100 μg/ml (Figure 3a). In addition, RAGE transcript levels were investigated by real-time PCR (Figure 3b), revealing a 1.5-fold upregulation after addition of 50 μg/ml CML-BSA compared to BSA ($P=0.057$).

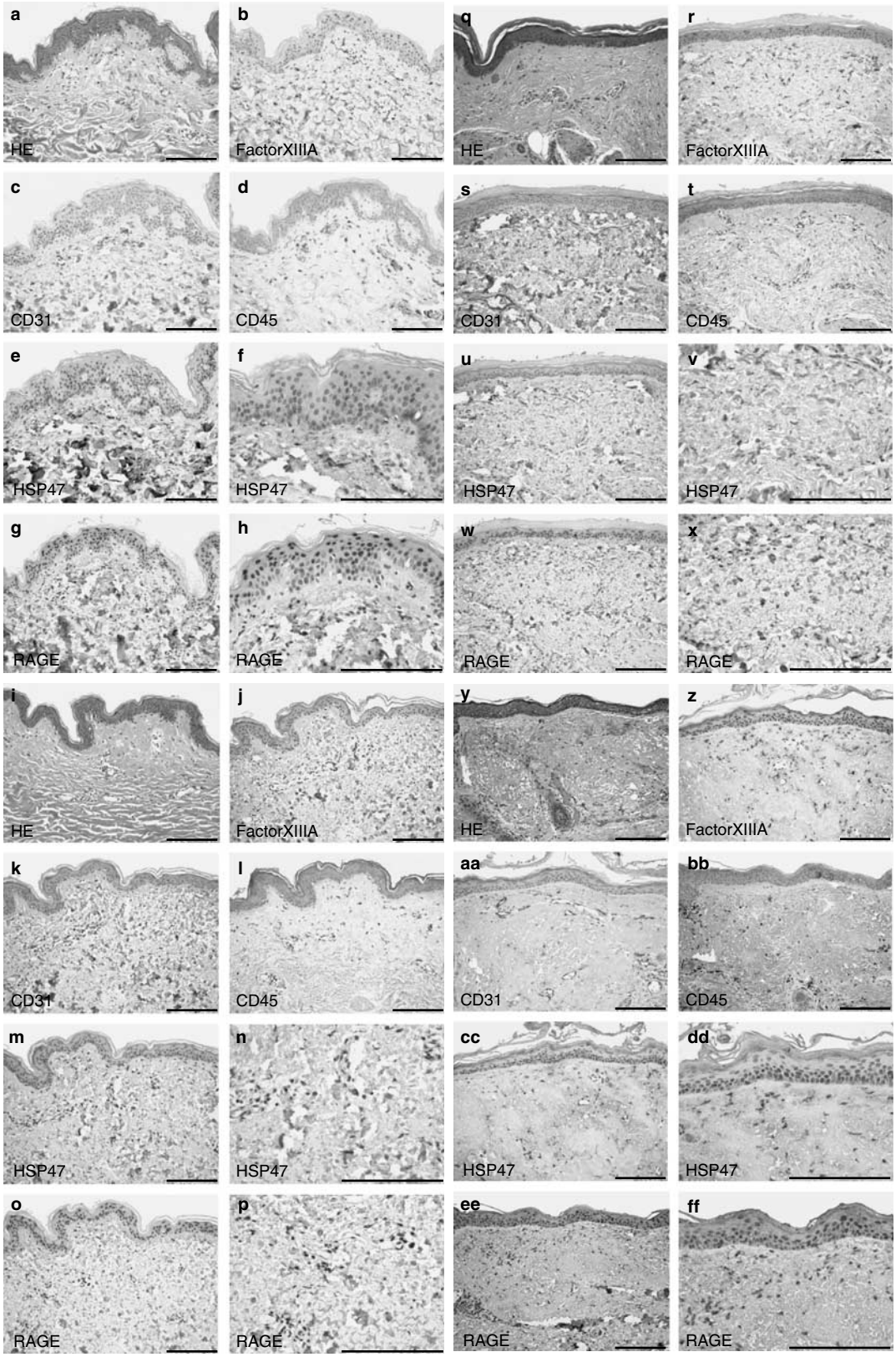

Figure 1. Expression of RAGE, HSP47, factor XIIIa, CD31, and CD45 in human skin. Hematoxylin–eosin stainings (**a**) showed basic morphological changes of the specimen due to aging and/or sun-aging. Factor (**b**) XIIIa, (**c**) CD31, (**d**) CD45, (**e/f**) HSP47, and (**g/h**) RAGE protein expression was investigated on consecutive sections of younger sun-protected (**a–h**, breast), older sun-protected (**i–p**, breast), older sun-protected (**q–x**, popliteal fossa), and older sun-exposed (**y–ff**, face) skin. Expression of RAGE was found mainly in the basal zone of the epidermis. RAGE was overexpressed in fibroblasts and dendrocytes close to areas of older skin damaged by sun exposure. Bar=200 μm.

Table 1. Semiquantification of immunohistochemical RAGE staining indicating the distribution pattern of RAGE

	Sun-protected breast (young)	Sun-protected breast (old)	Sun-protected knee (old)	Sun-exposed face (old)
Upper epidermis	+++	+/++	+/(++)	+/(++)
Lower epidermis	+/++	+++	+++	+++
Upper dermis	++	+	+	++/(+++)
Lower dermis	+	++	++	++

+ weak, ++ moderate, +++ strong intensity of RAGE; () indicates that this intensity level was only focally detected.

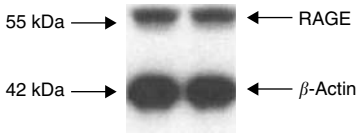

Figure 2. RAGE is expressed in HFFs. HFF were extracted, separated with 12% SDS-PAGE, and blotted using the monoclonal anti-RAGE antibody (1:100 dilution). Binding was visualized with a horseradish peroxidase-labeled secondary antibody. The lower band represents β-actin (monoclonal antibody, 1:5,000 dilution), which was used to control for protein loading. This is a representative blot from at least three independent experiments performed in duplicate.

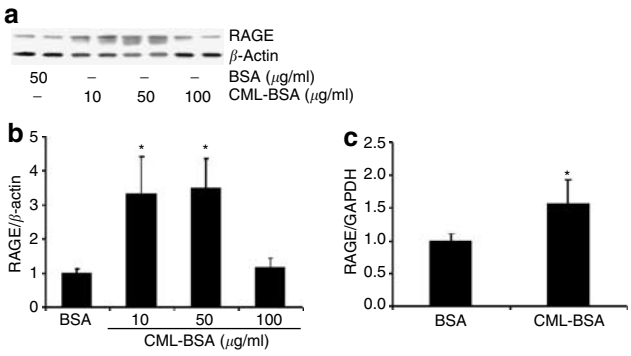

Figure 3. CML-BSA upregulates RAGE protein and mRNA expression in HFFs. (**a**) HFFs were treated with 50 μg/ml BSA as control and 10–100 μg/ml CML-BSA for 24 hours in starvation medium before extraction, separation, and blotting with the anti-RAGE antibody. Bars represent mean RAGE protein expression relative to β-actin (±SD) derived from three independent experiments performed in duplicate. (**b**) HFFs were incubated with 50 μg/ml BSA or CML-BSA for 24 hours in serum-free medium before RNA extraction and determination of RAGE mRNA expression by real-time PCR. (**c**) Bars represent mean RAGE mRNA expression relative to glyceraldehyde-3-phosphate dehydrogenase (GAPDH) mRNA (±SD) from two independent experiments performed in quadruplicate. $*P<0.05$ *versus* BSA.

When HFFs were exposed to increasing concentrations of TNF-α under serum-free conditions for 24 hours, RAGE protein expression was upregulated dose-dependently up to two-fold (Figure 4).

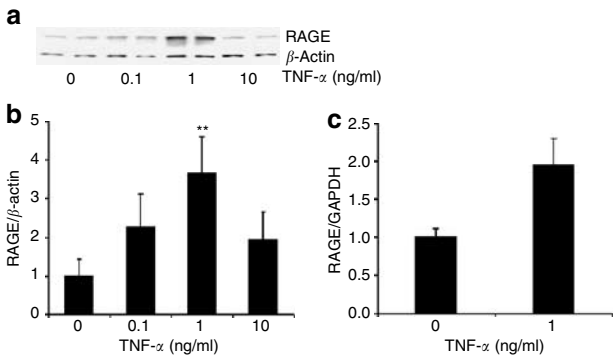

Figure 4. TNF-α upregulates RAGE protein and mRNA expression in HFFs. (**a**) HFF were treated with 0–10 ng/ml TNF-α for 24 hours in starvation medium before extraction, separation, and blotting with the anti-RAGE antibody. Bars represent mean RAGE protein expression relative to β-actin (±SD) derived from three independent experiments performed in duplicate. (**b**) HFFs were incubated with 0 or 1 ng/ml TNF-α for 24 hours in starvation medium before RNA extraction and determination of RAGE mRNA expression by real-time PCR. (**c**) Bars represent mean RAGE mRNA expression relative to GAPDH (±SD) from two independent experiments performed in quadruplicate. $**P<0.01$ *versus* 0 ng/ml TNF-α.

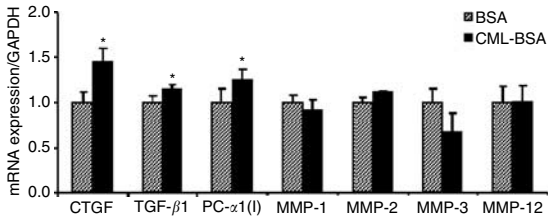

Figure 5. The specific RAGE ligand CML-BSA modulates ECM-related gene expression in HFFs. HFFs were treated with 50 μg/ml BSA or CML-BSA for 24 hours in starvation medium, extracted, and expression of CTGF, TGF-β1, PC-α1(I), MMP-1, MMP-2, MMP-3, and MMP-12 mRNAs was quantified by real-time PCR relative to GAPDH mRNA. Bars represent means ± SD derived from two independent experiments performed in quadruplicate. $*P<0.05$ *versus* BSA.

CML-BSA induces ECM-related gene expression

HFFs were incubated with CML-BSA or BSA as control, and mRNA expression was determined by real-time PCR (Figure 5). CML-BSA significantly upregulated CTGF, TGF-β1, and procollagen-α1(I) (PC-α1(I)) mRNA expression, whereas there was a trend for downregulation of MMP-3 mRNA and for upregulation of MMP-2 mRNA. Expression of MMP-1 and MMP-12 mRNA remained unchanged.

DISCUSSION

Fibroblasts play a central role in the turnover of the dermal extracellular matrix and are therefore involved in skin aging. AGEs were shown to accumulate on elastin and collagens and to bind to fibroblast membranes at concentrations of 2.5–40 mg/ml (Okano *et al.*, 2002). AGEs bind to several cellular receptors, including scavenger receptor class A and B, 80K-H phosphoprotein, galectin-3, lactoferrin, and specifically to RAGE. RAGE is expressed on several cells, and prominently on human microvascular endothelial cells

(Valencia *et al.*, 2004). In these cells, CML-ovalbumin stimulated NF-κB signaling mainly attributed to interactions with RAGE (Kislinger *et al.*, 1999). However, it is not known if and how far AGEs and RAGE may be involved in skin aging and ECM formation by dermal fibroblasts.

We could demonstrate for the first time that RAGE protein is highly expressed in human skin as shown by immunohistological analysis of younger *versus* older, sun-exposed *versus* sun-protected, and of fetal skin. In older patients (independent of sun exposure), RAGE was predominantly found in basal areas where skin regeneration occurs, compared to epidermal expression of RAGE in fetal skin and an intermediate expression pattern in older sun-protected skin. RAGE expression was increased in sun-exposed skin. We cannot exclude that anatomical differences between the largely sun-protected popliteal fossa and sun-exposed face may be partly responsible for the observed differences in RAGE expression, but for ethical reasons sun-protected and sun-exposed skin from the same location could not be obtained. However, we found no major differences in RAGE expression between sun-protected skin from older breast and knee, indicating that our results represent changes related to sun exposure and not local differences of expression. RAGE-positive cells were mainly keratinocytes, skin fibroblasts, dermal dendrocytes, and endothelial cells, but some expression was also observed in lymphocytes.

Keratinocytes, which represent 95% of epidermal cells, are metabolically highly active and secrete growth factors and cytokines, such as the proinflammatory cytokine TNF-α and interleukin-1, -6, and -8. During skin aging, such as through UV exposure, keratinocytes degenerate and release vascular endothelial growth factor and basic fibroblast growth factor, resulting in endothelial cell activation and enhanced angiogenesis, favoring a wound-healing response (Toyoda *et al.*, 2001). Endothelial cells also express MMP-1, -2, and -3, which degrade ECM components, and intercellular adhesion molecule-1, thus recruiting circulating macrophages and leukocytes, which secrete collagenases and myeloperoxidases that can degrade the ECM (Giacomoni and Rein, 2001).

As we found the highest RAGE expression in fibroblasts in the (upper) dermis, we performed cell culture experiments to show that HFFs express high levels of RAGE protein and mRNA. Based on its amino-acid sequence, RAGE has a molecular weight of approximately 42 kDa (Neeper *et al.*, 1992). The RAGE band in our studies migrated at about 57 kDa, similar to RAGE of hepatic stellate cells (Fehrenbach *et al.*, 2001; our own unpublished observation). Others previously reported RAGE as two distinct proteins migrating at around 30 and 50 kDa in the fibroblast cell line GM05757A (Owen *et al.*, 1998) or as a 50 kDa species in RAGE-transfected 293 cells (Neeper *et al.*, 1992). Furthermore, RAGE was detected in lung extracts at a size of 35 kDa (Brett *et al.*, 1993; Wautier *et al.*, 1994). These size differences are likely due to glycosylation of the extracellular domain (Neeper *et al.*, 1992) or to post-translational processing and proteolytic cleavage (Brett *et al.*, 1993; Yan *et al.*, 1994; Renard *et al.*, 1999).

RAGE expression in skin fibroblasts was inducible by CML-BSA, a specific RAGE ligand. AGEs accumulate on collagen and elastin in the skin, especially during the process of aging and after UV irradiation. In addition, we observed that the proinflammatory cytokine TNF-α, which is released after UV radiation to the skin and which is incriminated in skin aging (Yarosh *et al.*, 2000a, b), enhanced RAGE expression in HFF. RAGE induction through AGE-BSA and TNF-α was shown before in human umbilical vein endothelial cells (Tanaka *et al.*, 2000), and through AGE-BSA in normal rat kidney fibroblasts (Huang *et al.*, 2001).

Finally, we demonstrated that AGEs alter ECM-related gene expression in HFFs, which likely leads to enhanced turnover of the collagenous ECM in the skin. This addition of CML-BSA to HFFs significantly upregulated expression of CTGF, TGF-β1, and PC-α1(I), whereas MMP-2 expression was nonsignificantly induced. Expression of MMP-1, -3, and -12 remained largely unaffected by the addition of CML-BSA. CTGF induces ECM formation in fibroblasts, in part by mediating actions of the key profibrogenic cytokine TGF-β1 (Frazier *et al.*, 1996; Grotendorst, 1997). Induction of CTGF by 100 μg/ml AGE-BSA but not the RAGE-specific ligand CML-BSA in human dermal fibroblasts on a mRNA and protein basis has been reported previously (Twigg *et al.*, 2001). In line with our data, Huang *et al.* (2001) described that AGEs increased collagen production in normal rat kidney fibroblasts, whereas others found a decrease in a human fibroblasts cell line or no change in human skin fibroblasts (Owen *et al.*, 1998; Okano *et al.*, 2002). As we used the specific RAGE ligand CML-BSA, the divergent results may be due to stimulation of other AGE receptors than RAGE. Our overall findings show that in HFF, CML-BSA mildly stimulates interstitial collagen production (procollagen I, TGF-β1, CTGF), with a trend toward production of proteases, such as MMP-2, that destroy basement membranes. As UV radiation results in overall ECM degradation, especially of elastin, dermal fibroblasts and endothelial cells that were previously shown to release ECM proteolytic activity (Giacomoni and Rein, 2001) appear to play opposing roles with regard to skin aging and remodeling, with endothelial cells likely driving the degenerative changes of the dermis.

In conclusion, we could show that RAGE is highly expressed in skin and upregulated in sun-exposed skin. We could demonstrate that HFF highly express functional RAGE, and that a specific RAGE ligand upregulates RAGE expression and induces a mildly profibrogenic ECM remodeling in HFF.

MATERIALS AND METHODS

Materials

Antibodies against CD31 and CD45, biotinylated rabbit anti-mouse antibodies, non-immune mouse IgG1, streptavidin–biotin-complexed alkaline phosphatase, target retrieval solution, pH 6.0, and the catalyzed signal amplification system using biotinylated tyramids were supplied by Dako (Glostrup, Denmark). The antibodies against factor XIIIA (Ab-1) were from Lab Vision (Fremont, CA) and against HSP47 from Stressgen (Victoria, Canada). Avidin and biotin were

supplied by Vector Laboratories (Burlingame, CA). BSA, TNF-α, monoclonal anti-β-actin clone AC-15, goat anti-mouse IgG-peroxidase, and Fast Red were purchased from Sigma-Aldrich (Taufkirchen, Germany). DMEM was from Biochrom (Berlin, Germany). Fetal calf serum was purchased from PAA Laboratories (Linz, Austria). Monoclonal anti-RAGE antibody was produced as previously described (Srikrishna *et al*., 2002). The Bradford protein assay was from Bio-Rad Laboratories GmbH (Munich, Germany). Detoxi-Gel™ endotoxin-removing gel was from Pierce (Rockford, IL) and the limulus amebocyte lysate endotoxin test kit from Bio-Whittaker (Walkersville, MD). SuperScript™ II RNase reverse transcriptase and Novex® 12% tris-glycine precast gels without SDS were from Invitrogen (Karlsruhe, Germany). PeqGOLD RNAPure, dTTP, dGTP, dCTP, and dATP (100 mM each) were obtained from PeqLab Biotechnologie GmbH (Erlangen, Germany) and Oligo(dT)$_{15}$ primer, random primers, and RNasin® ribonuclease inhibitor from Promega (Madison, WI). LightCycler fast start DNA master hybridization probes, LightCycler capillaries, LightCycler instrument, and Complete™ proteinase inhibitor cocktail were from Roche Diagnostics (Mannheim, Germany). The enhanced chemiluminescence Western blotting detection reagents were from Amersham Pharmacia Biotech (Freiburg, Germany) and nitrocellulose membranes from Schleicher & Schuell GmbH (Dassel, Germany). The mycoplasma-test Venor GeM® was purchased from Minerva Biolabs GmbH (Berlin, Germany). Citric acid monohydrate was from Merck (Darmstadt, Germany).

Skin samples and histological analysis

Informed written consent of patients was obtained before tissue resection and the study was conducted according to the Declaration of Helsinki Principles. All studies were approved by the ethical committee of the University of Erlangen-Nuernberg. To evaluate age dependency of RAGE expression, six skin samples from mammary reductions of younger patients (average age 32.2±5.6 years) and one sample from fetal skin (week 19 of gestation, from autopsy) were compared to six skin samples from older, non-exposed mammary tissue derived from breast ablation due to cancer (average age 73.6±7.3 years). To evaluate sun exposure-dependent RAGE expression, six skin samples derived from non-exposed popliteal fossa of above-knee amputations due to arterial occlusive disease (average age 74.5±11.6 years) were compared to 10 skin samples derived from sun-exposed healthy resection margins of surgically excised facial tumors (average age 67.0±12.1 years) (Table 2). Specimens were immediately fixed in 10% buffered formalin. After embedding in paraffin, 5 μm sections were cut and stored at room temperature. Routine hematoxylin–eosin staining was used to evaluate basic histomorphology of the specimens.

For immunohistology, consecutive sections were deparaffinized using graded alcohol. To prevent nonspecific binding of antibodies, sections were blocked with avidin and biotin. Sections were incubated overnight at room temperature using monoclonal antibodies to RAGE (1:50), CD45 (1:50), and HSP47 (1:100) (all pretreated with target retrieval solution, pH 6.0, for 30 s at 120°C), factor XIIIA Ab-1 (1:500), and CD31 (1:20) (both pretreated with citrate buffer, pH 6.0, for 60 s at 120°C: 10.5 g citric acid monohydrate in 5 l H_2O, pH 6.0), followed by biotinylated rabbit anti-mouse IgG and streptavidin–biotin alkaline phosphatase. Sections were developed using Fast Red and nuclei were counterstained

Table 2. Characterization of patient tissues

Age	Gender	Location	Operation due to
(a) Specimens of younger, sun-protected skin			
36[1]	F	Breast[2]	Mammary reduction
28	F	Breast[2]	Mammary reduction
34	F	Breast[2]	Mammary reduction
38	F	Breast[2]	Mammary reduction
25	F	Breast[2]	Mammary reduction
19th week of gestation	F	Abdomen	Intrauterine death
(b) Specimens of older, sun-protected skin			
75	F	Breast[2]	Breast ablation due to cancer
79	F	Breast[2]	Breast ablation due to cancer
76[1]	F	Breast[2]	Breast ablation due to cancer
78	F	Breast[2]	Breast ablation due to cancer
59	F	Breast[2]	Breast ablation due to cancer
75	F	Breast[2]	Breast ablation due to cancer
(c) Specimens of older, sun-protected skin			
92	F	Popliteal fossa	Arterial occlusive disease (above-knee amputation)
63	M	Popliteal fossa	Arterial occlusive disease (above-knee amputation)
86	F	Popliteal fossa	Arterial occlusive disease (above-knee amputation)
67	M	Popliteal fossa	Arterial occlusive disease (above-knee amputation)
69	M	Popliteal fossa	Arterial occlusive disease (above-knee amputation)
70[1]	F	Popliteal fossa	Arterial occlusive disease (above-knee amputation)
(d) Specimens of older, sun-exposed skin			
65	F	Face, jowl	Actinic keratosis with dysplasia
57	M	Face, front	Squamous cell carcinoma
91	M	Face, jowl	Squamous cell carcinoma
65	F	Face, jowl	Actinic keratosis with dysplasia
62[1]	F	Face, ear	Seborrheic keratosis
62	M	Face, alar wing of the nose	Basal cell carcinoma
65	F	Face, jowl	Actinic keratosis with dysplasia
87	M	Face, front	Squamous cell carcinoma
63	M	Face, alar wing of the nose	Basal cell carcinoma
53	F	Face, ear	Seborrheic keratosis

[1]Displayed in Figure 1.
[2]Mainly from the lateral quadrant.

with hematoxylin. RAGE was detected with the catalyzed signal amplification system as described (van Gijlswijk *et al.*, 1996) using biotinylated tyramin, which was applied after the streptavidin–biotin–peroxidase complex. The biotinylated tyramin was then enzymatically cleaved, resulting in localized precipitation of biotin, followed by detection with the streptavidin–biotin–alkaline phosphatase complex. In control experiments, non-immune mouse IgG1 and phosphate-buffered saline replaced primary and secondary antibodies, respectively, with the same processing of the samples as described above. All controls showed no stainings (data not shown).

In order to evaluate the expression levels of RAGE inside the dermis, we used semiquantitative analysis with a scale from weak (+), to moderate (++) and strong (+++) intensity by investigating 10 different areas per specimen.

Synthesis of CML-BSA

BSA (2.65 mM) and $NaCNBH_3$ (0.45 M) were dissolved in 10 ml 0.2 M phosphate buffer, pH 7.8, followed by addition of 0.255 M glyoxylic acid and incubation at room temperature for 48 hours. The reaction product was dialyzed against water and lyophilized. Control BSA was handled the same way, but without the addition of glyoxylic acid. Protein concentrations were adjusted by the Bio-Rad protein assay and endotoxin was removed with endotoxin-removing gel and the residual endotoxin measured with the limulus amebocyte lysate test (endotoxin concentration in both preparations <0.02 ng/ml). Glycation of CML-BSA was determined with the 2,4,6-trinitrobenzenesulfonic acid assay (Fields, 1972), yielding a glycation rate of 36.5%.

Cell culture

HFFs were kindly provided by Dr M. Marschall (Institute for Virology, University of Erlangen-Nuernberg, Germany). Cells were maintained in 75 cm^2 cell culture flasks in a humidified atmosphere with 5% CO_2 at 37°C and DMEM supplemented with 10% heat-inactivated fetal calf serum and 1% penicillin (100 IU/ml) and streptomycin (100 μg/ml). Only cells that tested mycoplasma-negative and that were prior to their 15th passage were used for experiments.

Treatment of cells and protein extraction

HFFs were seeded at 20,000 cells per well in 24-well plates and when reaching a preconfluent stage were incubated in 500 μl starvation medium (DMEM containing 1% penicillin/streptomycin and 0.125% fetal calf serum) for 24 hours. Then, cells were treated with 10–100 μg/ml CML-BSA, 50 μg/ml control BSA, or 0–10 ng/ml TNF-α for 24 hours, followed by washing with ice-cold phosphate-buffered saline and lysis in a buffer containing 0.06 M Tris, pH 6.8, 2% SDS, 8% glycerol, 1 M urea, and 10 mg/ml dithiothreitol. Lysates were heated at 95°C for 5 min and stored at −20°C until further use.

SDS-PAGE and Western blotting

Lysates were subjected to SDS-PAGE and blotted onto nitrocellulose membranes. Membranes were blocked in 3% BSA and incubated overnight with monoclonal anti-RAGE (1:100) and anti-β-actin (1:5,000) antibodies, followed by anti-mouse IgG conjugated to peroxidase (1:5,000). Bands were visualized by enhanced chemiluminescence and quantified densitometrically using the BioDoc Analyzer (Biometra, Goettingen, Germany).

Real-time PCR for ECM-related gene expression

RNA of treated cells was extracted using peqGOLD RNAPure™ according to the manufacturer's recommendations. Extracted RNA was resuspended in 18 μl of RNase-free water and 2 μl each was used to measure the RNA concentration by UV spectroscopy at 260 nm and to determine RNA integrity on an agarose gel. The solubilized RNA was frozen immediately and stored at −80°C until use. A 1 μg portion of RNA was reverse-transcribed into cDNA using 100 pmol oligo-dT, 50 pmol random primer, and 100 U Superscript II following the recommendations of the supplier. The cDNA was stored at −20°C until use.

Table 3. Sequences of human primers and probes used for real-time PCR

mRNA	Oligonucleotide	Sequence (5′→3′)
GAPDH	GAPDH sense	CCA CAT CGC TCA GAC ACC AT
	GAPDH antisense	CCA GGC CAA TAC G
	GAPDH probe	AAG GTG AAG GTC GGA GTC AAC GGA TTT G
RAGE	RAGE sense	ACC AGG GAA CCT ACA GCT GTG T
	RAGE antisense	TAG AGT TCC CAG CCC TGA TCC T
	RAGE probe	CAT CAG CAT CAT CGA ACC AGG CGA GGA
CTGF	CTGF sense	AAC CGC AAG ATC GGC GT
	CTGF antisense	CCG TAC CAC CGA AGA TGC A
	CTGF probe	TGC ACC GCC AAA GAT GGT GCT C
TGF-β	TGF-β sense	TGC GTC TGC TGA GGC TCA A
	TGF-β antisense	TTG CTG AGG TAT CGC CAG GA
	TGF-β probe	ACG TGG AGC TGT ACC AGA AAT ACA GCA ACA
PC-α1(I)	PC-α1(I) sense	CAG AAG AAC TGG TAC ATC AGC AAG A
	PC-α1(I) antisense	GTC AGC TGG ATG GCC ACA T
	PC-α1(I) probe	ACC GAT GGA TTC CAG TTC GAG TAT GGC
MMP-1	MMP-1 sense	CAG TGG TGA TGT TCA GCT AGC TCA
	MMP-1 antisense	GCC GAT GGG CTG GAC A
	MMP-1 probe	CAT CCA AGC CAT ATA TGG ACG TTC CCA AA
MMP-2	MMP-2 sense	GAG GAC TAC GAC CGC GAC AA
	MMP-2 antisense	TTG TTG CCC AGG AAA GTG AAG
	MMP-2 probe	TCT GCC CTG AGA CCG CCA TGT CC
MMP-3	MMP-3 sense	GTT CCG CCT GTC TCA AGA TGA
	MMP-3 antisense	TAC CCA CGG AAC CTG TCC C
	MMP-3 probe	TAA ATG GCA TTC AGT CCC TCT ATG GAC CTC C
MMP-12	MMP-12 sense	CGC CTC TCT GCT GAT GAC ATA C
	MMP-12 antisense	TCA GTC CCT GTA TGG AGA CCC AAA AGA GAA
	MMP-12 probe	CAG GAT TTG GCA AGC GTT G

Real-time RT-PCR was performed on a LightCycler (Roche, Mannheim, Germany) using the TaqMan principle in a reaction volume of 15 μl (Dotsch *et al.*, 2001). The mix included FastStart *Taq* DNA polymerase, dNTP mix, reaction buffer, 3 mM $MgCl_2$, 2 μM each of the primers, and 0.5 μM of the probe. After pipetting 13.5 μl of this mixture into LightCycler capillaries, 1.5 μl template cDNA was added. The capillaries were sealed and placed into the thermal chamber of the LightCycler. Samples were amplified with a precycling step at 95°C for 10 min, followed by 40 cycles of denaturation at 95°C for 0.1 s, annealing at 60°C for 15 s, and extension at 72°C for 6 s. Data were analyzed according to a standard curve generated from a dilution series of a mixture of representative samples. For normalization of differences in RNA amounts and efficiencies in the reverse transcription reactions, the housekeeping gene GAPDH was co-amplified.

The specific sense and antisense oligonucleotide primers and probes (Table 3) were designed based on published sequences. Probes were labeled with a reporter dye (FAM, spanning exon boundaries to avoid co-amplification of genomic DNA) at the 5′ end and a quencher dye (TAMRA) at the 3′ end and were synthesized at MWG Biotech AG (Ebersberg, Germany).

Statistics

All statistical analyses were performed using Microsoft® EXCEL 2000. The statistical significance of differences was determined using the unpaired Student's *t*-test. Differences with *P*-values <0.05 were considered statistically significant. All graphs represent the mean $\pm$ standard deviation (SD) and were performed at least in triplicate.

CONFLICT OF INTEREST

The authors state no conflict of interest.

ACKNOWLEDGMENTS

We thank Christa Winkelmann, Gisela Weber, and Kunigunde Herbig (Department of Pathology, University of Erlangen-Nuernberg, Germany) for their expert technical assistance and Manfred Marschall (Institute for Clinical and Molecular Virology, University of Erlangen-Nuernberg, Germany) for supplying the HFF. In addition, we thank Monika Pischetsrieder (Institute of Pharmacy and Food Chemistry, University of Erlangen-Nuernberg, Germany) for contributing to the concept of this study and fruitful discussion of the results. This work was in part supported by a grant from the Johannes and Frieda Marohn-Foundation of the University of Erlangen-Nuernberg, Germany.

REFERENCES

Brenneisen P, Oh J, Wlaschek M, Wen J, Briviba K, Hommel C *et al.* (1996) Ultraviolet B wavelength dependence for the regulation of two major matrix-metalloproteinases and their inhibitor TIMP-1 in human dermal fibroblasts. *Photochem Photobiol* 64:649–57

Brenneisen P, Wlaschek M, Schwamborn E, Schneider LA, Ma W, Sies H *et al.* (2002) Activation of protein kinase CK2 is an early step in the ultraviolet B-mediated increase in interstitial collagenase (matrix metalloproteinase-1; MMP-1) and stromelysin-1 (MMP-3) protein levels in human dermal fibroblasts. *Biochem J* 365:31–40

Brett J, Schmidt AM, Yan SD, Zou YS, Weidmann E, Pinsliy D *et al.* (1993) Survey of the distribution of a newly characterized receptor for advanced glycation end products in tissues. *Am J Pathol* 143:1699–712

Burgeson RE (1982) Genetic heterogeneity of collagens. *J Invest Dermatol* 79:25s–30s

Chandler S, Cossins J, Lury J, Wells G (1996) Macrophage metalloelastase degrades matrix and myelin proteins and processes a tumour necrosis factor-alpha fusion protein. *Biochem Biophys Res Commun* 228: 421–9

Dotsch J, Hogen N, Nyul Z, Hanze J, Knerr I, Kirschbaum M *et al.* (2001) Increase of endothelial nitric oxide synthase and endothelin-1 mRNA expression in human placenta during gestation. *Eur J Obstet Gynecol Reprod Biol* 97:163–7

Dyer DG, Dunn JA, Thorpe SR, Bailie KE, Lyons TJ, McCance DR *et al.* (1993) Accumulation of Maillard reaction products in skin collagen in diabetes and aging. *J Clin Invest* 91:2463–9

Fehrenbach H, Weiskirchen R, Kasper M, Gressner AM (2001) Up-regulated expression of the receptor for advanced glycation end products in cultured rat hepatic stellate cells during transdifferentiation to myofibroblasts. *Hepatology* 34:943–52

Fields R (1972) The rapid determination of amino groups with TNBS. *Methods Enzymol* 15:464–8

Frazier K, Williams S, Kothapalli D, Klapper H, Grotendorst GR (1996) Stimulation of fibroblast cell growth, matrix production, and granulation tissue formation by connective tissue growth factor. *J Invest Dermatol* 107:404–11

Giacomoni PU, Rein G (2001) Factors of skin ageing share common mechanisms. *Biogerontology* 2:219–29

Gronski Jr TJ, Martin RL, Kobayashi DK, Walsh BC, Holmann MC, Huber M *et al.* (1997) Hydrolysis of a broad spectrum of extracellular matrix proteins by human macrophage elastase. *J Biol Chem* 272:12189–94

Grotendorst GR (1997) Connective tissue growth factor: a mediator of TGF-β action on fibroblasts. *Cytokine Growth Factor Rev* 8:171–9

Huang JS, Guh JY, Chen HC, Hung WC, Lai YH, Chuang LY (2001) Role of receptor for advanced glycation end-product (RAGE) and the JAK/STAT-signaling pathway in AGE-induced collagen production in NRK-49F cells. *J Cell Biochem* 81:102–13

Jeanmaire C, Danoux L, Pauly G (2001) Glycation during human dermal intrinsic and actinic ageing: an *in vivo* and *in vitro* model study. *Br J Dermatol* 145:10–8

Kislinger T, Fu C, Huber B, Qu W, Taguchi A, Du Yan S *et al.* (1999) N(epsilon)-(carboxymethyl)lysine adducts of proteins are ligands for receptor for advanced glycation end products that activate cell signaling pathways and modulate gene expression. *J Biol Chem* 274:31740–9

Kligman LH, Kligman AM (1986) The nature of photoaging: its prevention and repair. *Photodermatology* 3:215–27

Koivukangas V, Kallioinen M, Autio-Harmainen H, Oikarinen A (1994) UV irradiation induces the expression of gelatinases in human skin *in vivo*. *Acta Derm Venereol* 74:279–82

Lovell CR, Smolenski KA, Duance VC, Light ND, Young S, Dyson M (1987) Type I and III collagen content and fibre distribution in normal human skin during ageing. *Br J Dermatol* 117:419–28

Meng J, Sakata N, Imanaga Y, Takebayashi S, Nagai R, Horiuchi S (2001) Carboxymethyllysine in dermal tissues of diabetic and nondiabetic patients with chronic renal failure: relevance to glycoxidation damage. *Nephron* 88:30–5

Mizutari K, Ono T, Ikeda K, Kayashima K, Horiuchi S (1997) Photo-enhanced modification of human skin elastin in actinic elastosis by N(epsilon)-(carboxymethyl)lysine, one of the glycoxidation products of the Maillard reaction. *J Invest Dermatol* 108:797–802

Monnier VM, Bautista O, Kenny D, Sell DR, Fogarty J, Dahms W *et al.* (1999) Skin collagen glycation, glycoxidation, and crosslinking are lower in subjects with long-term intensive *versus* conventional therapy of type 1 diabetes: relevance of glycated collagen products *versus* HbA1c as markers of diabetic complications. DCCT Skin Collagen Ancillary Study Group. Diabetes Control and Complications Trial. *Diabetes* 48:870–80

Monnier VM, Kohn RR, Cerami A (1984) Accelerated age-related browning of human collagen in diabetes mellitus. *Proc Natl Acad Sci USA* 81:583–7

Neeper M, Schmidt AM, Brett J, Yan SD, Wang F, Pan YC *et al.* (1992) Cloning and expression of a cell surface receptor for advanced glycation end products of proteins. *J Biol Chem* 267:14998–5004

Okano Y, Masaki H, Sakurai H (2002) Dysfunction of dermal fibroblasts induced by advanced glycation end-products (AGEs) and the contribu-

tion of a nonspecific interaction with cell membrane and AGEs. *J Dermatol Sci* 29:171–80

Owen Jr WF, Hou FF, Stuart RO, Kay J, Boyce J, Chertow GM *et al.* (1998) Beta 2-microglobulin modified with advanced glycation end products modulates collagen synthesis by human fibroblasts. *Kidney Int* 53:1365–73

Renard C, Chappey O, Wautier MP, Nagashima M, Morser J, Scherrmann JM *et al.* (1999) The human and rat recombinant receptors for advanced glycation end products have a high degree of homology but different pharmacokinetic properties in rats. *J Pharmacol Exp Ther* 290:1458–66

Schnider SL, Kohn RR (1980) Glucosylation of human collagen in aging and diabetes mellitus. *J Clin Invest* 66:1179–81

Schnider SL, Kohn RR (1981) Effects of age and diabetes mellitus on the solubility and nonenzymatic glucosylation of human skin collagen. *J Clin Invest* 67:1630–5

Shipley JM, Wesselschmidt RL, Kobayashi DK, Ley TJ, Shapiro SD (1996) Metalloelastase is required for macrophage-mediated proteolysis and matrix invasion in mice. *Proc Natl Acad Sci USA* 93:3942–6

Srikrishna G, Huttunen HJ, Johansson L, Weigle B, Yamaguchi Y, Rauvala H *et al.* (2002) N-glycans on the receptor for advanced glycation end products influence amphoterin binding and neurite outgrowth. *J Neurochem* 80:998–1008

Tanaka N, Yonekura H, Yamagishi S, Fujimori H, Yamamoto Y, Yamamoto H (2000) The receptor for advanced glycation end products is induced by the glycation products themselves and tumor necrosis factor-alpha through nuclear factor-kappa B, and by 17beta-estradiol through Sp-1 in human vascular endothelial cells. *J Biol Chem* 275:25781–90

Toyoda M, Nakamura M, Luo Y, Morohashi M (2001) Ultrastructural characterization of microvasculature in photoaging. *J Dermatol Sci* 27(Suppl 1):S32–41

Twigg SM, Chen MM, Joly AH, Chakrapani SD, Tsubaki J, Kim HS *et al.* (2001) Advanced glycosylation end products up-regulate connective tissue growth factor (insulin-like growth factor-binding protein-related protein 2) in human fibroblasts: a potential mechanism for expansion of extracellular matrix in diabetes mellitus. *Endocrinology* 142:1760–9

Valencia JV, Mone M, Koehne C, Rediske J, Hughes TE (2004) Binding of receptor for advanced glycation end products (RAGE) ligands is not sufficient to induce inflammatory signals: lack of activity of endotoxin-free albumin-derived advanced glycation end products. *Diabetologia* 47:844–52

van Gijlswijk RP, Wiegant J, Raap AK, Tanke HJ (1996) Improved localization of fluorescent tyramides for fluorescence *in situ* hybridization using dextran sulfate and polyvinyl alcohol. *J Histochem Cytochem* 44: 389–92

Wautier JL, Guillausseau PJ (2001) Advanced glycation end products, their receptors and diabetic angiopathy. *Diabetes Metab* 27:535–42

Wautier JL, Wautier MP, Schmidt AM, Anderson GM, Hori O, Zoukourian C *et al.* (1994) Advanced glycation end products (AGEs) on the surface of diabetic erythrocytes bind to the vessel wall via a specific receptor inducing oxidant stress in the vasculature: a link between surface-associated AGEs and diabetic complications. *Proc Natl Acad Sci USA* 91:7742–6

Wondrak GT, Roberts MJ, Jacobson MK, Jacobson EL (2002) Photosensitized growth inhibition of cultured human skin cells: mechanism and suppression of oxidative stress from solar irradiation of glycated proteins. *J Invest Dermatol* 119:489–98

Wulf HC, Sandby-Moller J, Kobayasi T, Gniadecki R (2004) Skin aging and natural photoprotection. *Micron* 35:185–91

Yan SD, Schmidt AM, Anderson GM, Zhang I, Brett J, Zou YS *et al.* (1994) Enhanced cellular oxidant stress by the interaction of advanced glycation end products with their receptors/binding proteins. *J Biol Chem* 269:9889–97

Yarosh D, Both D, Kibitel J, Anderson C, Elmets C, Brash D *et al.* (2000a) Regulation of TNFalpha production and release in human and mouse keratinocytes and mouse skin after UV-B irradiation. *Photodermatol Photoimmunol Photomed* 16:263–70

Yarosh DB, Cruz PD, Dougherty I, Bizios N, Kibitel J, Goodtzova K *et al.* (2000b) FRAP DNA-dependent protein kinase mediates a late signal transduced from ultraviolet-induced DNA damage. *J Invest Dermatol* 114:1005–10